

DCE-MRI of Human Brain Tumors Using Gadoteridol and Ferumoxytol

J. M. Njus¹, C. G. Varallyay², J. W. Grinstead³, X. Li¹, C. S. Springer, Jr.¹, E. A. Neuwelt², and W. D. Rooney¹

¹Advanced Imaging Research Center, Oregon Health and Science University, Portland, OR, United States, ²Department of Neurology, Oregon Health and Science University, Portland, Oregon, United States, ³Siemens Medical Solutions, Inc, Portland, Oregon, United States

Introduction

Dynamic contrast-enhanced (DCE) MRI techniques are widely used for characterizing blood-brain barrier (BBB) permeability and fractional brain tissue volumes.¹⁻⁶ Low molecular weight contrast reagents (CR), typified by the monomeric Gd(III) chelates, are used almost exclusively for these applications in human subjects. A characteristic of the Gd(III) CR is rapid extravasation in areas with BBB compromise, which allows permeability measurements to be made quickly and with good fidelity. Another important biomarker accessible to DCE-MRI is the cerebral blood volume fraction (v_b), which is often markedly increased in aggressive tumors.⁷⁻¹⁰ However, in regions of high BBB permeability, accurate v_b quantification can be difficult or impossible using the low molecular weight Gd(III) CRs. This difficulty may be overcome using macromolecular iron oxide (FeO) CRs,¹¹⁻¹⁴ such as ferumoxytol,^{13,14} which remain essentially intravascular at short times after administration; even in malignant brain tumors,^{11,12} but extravasation is evident after 24 hr.¹⁵ Clearly, the potential for DCE-MRI with FeO CR to quantify brain tumor v_b values would be important for understanding tumor pathology and for evaluation of emerging cancer therapies. In this study, we demonstrate a simple, yet novel mapping method using a Gd and an FeO CR serially to quantify cerebral blood volume and BBB permeability in human glioblastoma multiforme (GBM). To our knowledge, this is the first study using ferumoxytol to obtain quantitative cerebral blood volume and BBB permeability maps.

Methods

Eight GBM subjects (six men, two women) provided informed consent before participating in this study. All MR data were collected using a 3T Siemens TIM instrument. A body transmit and a 12-channel phased-array head receive RF coil pair was used. $^1\text{H}_2\text{O}$ R_1 [$\equiv 1/T_1$] data were collected using a fast (~4 minute full-volume acquisition) 2D gradient-echo EPI sequence with non-selective inversion recovery pulses.¹⁶ Twenty-four inversion times (TI) were sampled post-inversion maps with a $(128)^2$ matrix over a $(256 \text{ mm})^2$ FOV. Parametric R_1 maps were produced by voxel-wise fitting of the magnitude images to the signal intensity, $S(\text{TI}) = |S_0(1 - 2e^{-\text{TI}R_1})|$, using a gradient expansion algorithm. R_1 data sets were collected prior to, and at four times (measured at acquisition midpoints) after, CR injection. A 0.1 mmol/kg gadoteridol (ProHance, Bracco) dose was used and 2-4 mg/kg ferumoxytol (Advanced Magnetix Inc) dose was used. The Gd- and FeO- based CRs were each injected at rates of 3 mL/s, using a power injector. Each subject was examined on three consecutive days: the Gd CR was administered on day one, the FeO CR was used on day two, and 24 hr post-FeO R_1 map (a fifth FeO CR time point) was collected on day three. Cerebral blood volume and BBB permeability maps were determined as those of the p_b (blood water mole fraction: proportional to v_b), K^{trans} (FeO CR), and K^{trans} (Gd CR) values (K^{trans} is the volume transfer constant of CR across the BBB) quantities.¹⁻³ Two compartment (for CR and for water) models, which account for equilibrium intercompartmental water molecule exchange, were used. For each subject, the longitudinal R_1 maps (sec^{-1}) associated with both the pre- and post-CR sessions were co-registered to a common reference image set using a rigid-body transformation technique. MATLAB 7.0 (MathWorks) was used to obtain the p_b and K^{trans} maps *via* multi-parameter fittings.¹⁻⁶

Results

Figure 1 shows a 24 hr post-FeO T_2 -w (TSE TE88/TR9000/ETL9) axial anatomical image of a plane containing a GBM tumor, which is enclosed within a rectangular region-of-interest (ROI) (A). In the ROI are notable hypointense regions caused by intravenous FeO CR. Relatively large blood vessels within the ROI are marked (labeled arrows: 1-3). To the right are three ROI parametric maps: p_b (B), K^{trans} (FeO CR) (C), and K^{trans} (Gd CR) (D).

Discussion

In **Figure 1**, the notable hypointensities in the T_2 -w image (A) located within and/or near the periphery of the brain tumor (i.e. arrows 1, 3) likely represent increased angiogenic vascularization.¹⁷ Support of this hypothesis is available from the ROI blood water fraction map (B). The hypointensity pattern in the T_2 -w image can be seen as hyperintensity in the p_b map; verifying the assumption that the FeO CR is essentially strictly intravascular. The ferumoxytol BBB permeability (C) is very slow (i.e. maximum K^{trans} (FeO CR) values of $\sim 10^{-5} \text{ min}^{-1}$), and the assumption that this K^{trans} is effectively zero in malignant GBM tumors is quite justified. The ferumoxytol K^{trans} values could only be quantified because of the long plasma half-life of ferumoxytol (~14 hrs), and R_1 measurement at 24 hrs post-ferumoxytol administration. However, the Gd CR BBB permeability (D) in this GBM tumor is very high (K^{trans} (Gd CR) values of $\sim 10^{-2} \text{ min}^{-1}$). Therefore, while Gd CRs may be very useful for examining GBM BBB disruption, obtaining reliable p_b maps is substantially easier using ferumoxytol.

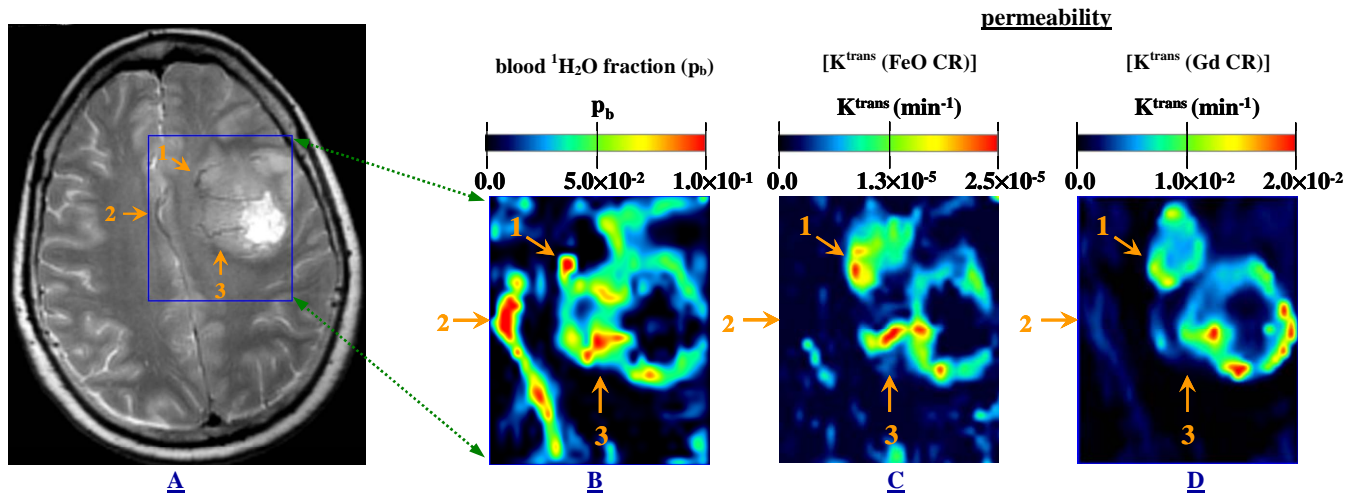


Figure 1. A T_2 -weighted (T_2 -w) post-FeO anatomical image (A) of a 58 yr. old female GBM subject is shown with a superimposed rectangular region-of-interest (ROI) and qualitative visual markers (1-3). There are three parametric ROI maps: B) blood water fraction (p_b); C) K^{trans} (FeO CR); and D) K^{trans} (Gd CR).

Grant Support

R01 NS053468, SAIC/NCI Contract #26XS293, NIH NS 040801

References

1. Tofts, et al., *JMRI* 10:223-232 (1999).
2. Landis, et al., *MRM* 44:563-574 (2000).
3. Yankeelov, et al., *MRM* 50:1151-1169 (2003).
4. Rooney, et al., *PISMRM* 11:2188 (2003).
5. Rooney, et al., *PISMRM* 11:1390 (2004).
6. Njus, et al., *PISMRM* 15:2193 (2007).
7. Li, et al., *JMRI* 12:347-357 (2000).
8. Pathak, et al., *MRM* 46:735-747 (2001).
9. Johnson, et al., *MRM* 51:961-968 (2004).
10. Atkins, et al., *Br. J. Surg.* 93:992-1000 (2006).
11. Neuwelt, et al., *Neuropath. Applied Neurobiol.* 30:456-471 (2004).
12. Murillo, et al., *Therapy* 2:871-882 (2005).
13. Simon, et al., *Ivest. Radiol.* 41:45-51 (2006).
14. Priest, et al., *MRI* 24:1287-1293 (2006).
15. Neuwelt, et al., *Neurosurgery* 60:601-612 (2007).
16. Clare, et al., *MRM* 45:630-634 (2001).
17. Barrett, *JMRI* 26:235-249 (2007).